AGU PUBLICATIONS

JGR

Journal of Geophysical Research: Space Physics

RESEARCH ARTICLE

10.1002/2013JA019115

Key Points:
- T_p in small transients is not much less than the expected proton temperature
- Low T_p is not a robust signature of small transients
- Force-free modeling of flux rope small transients may be inappropriate

Correspondence to:
W. Yu,
charlie.farrugia@unh.edu

Citation:
Yu, W., et al. (2014), A statistical analysis of properties of small transients in the solar wind 2007–2009: STEREO and Wind observations, *J. Geophys. Res. Space Physics*, *119*, 689–708, doi:10.1002/2013JA019115.

Received 12 JUN 2013
Accepted 22 DEC 2013
Accepted article online 27 DEC 2013
Published online 12 FEB 2014

A statistical analysis of properties of small transients in the solar wind 2007–2009: STEREO and Wind observations

W. Yu[1], C. J. Farrugia[1], N. Lugaz[1], A. B. Galvin[1], E. K. J. Kilpua[2], H. Kucharek[1], C. Möstl[3,4], M. Leitner[3], R. B. Torbert[1], K. D. C. Simunac[1], J. G. Luhmann[4], A. Szabo[5], L. B. Wilson III[5], K. W. Ogilvie[5], and J.-A. Sauvaud[6]

[1]Space Science Center and Department of Physics, University of New Hampshire, Durham, New Hampshire, USA, [2]Department of Physics, Division of Geophysics and Astronomy, University of Helsinki, Helsinki, Finland, [3]Institute of Physics, University of Graz, Graz, Austria, [4]Space Science Laboratories, University of California, Berkeley, California, USA, [5]NASA/Goddard Space Flight Center, Greenbelt, Maryland, USA, [6]Institut de Recherche en Astrophysique et Planetologie (CNRS-UPS), University of Toulouse, Toulouse, France

Abstract We present a comprehensive statistical analysis of small solar wind transients (STs) in 2007–2009. Extending work on STs by Kilpua et al. (2009) to a 3 year period, we arrive at the following identification criteria: (i) a duration < 12 h, (ii) a low proton temperature and/or a low proton beta, and (iii) enhanced field strength relative to the 3 year average. In addition, it must have at least one of the following: (a) decreased magnetic field variability, (b) large, coherent rotation of the field vector, (c) low Alfvén Mach number, and (d) T_e/T_p higher than the 3 year average. These criteria include magnetic flux ropes. We searched for STs using Wind and STEREO data. We exclude Alfvénic fluctuations. Case studies illustrate features of these configurations. In total, we find 126 examples, $\sim 81\%$ of which lie in the slow solar wind ($\lesssim 450$ km s^{-1}). Many start or end with sharp field and flow gradients/discontinuities. Year 2009 had the largest number of STs. The average ST duration is $\sim$ 4.3 h, $75\% < 6$ h. Comparing with interplanetary coronal mass ejections (ICMEs) in the same solar minimum, we find the major difference to be that T_p in STs is not significantly less than the expected T_p. Thus, whereas a low T_p is generally considered a very reliable signature of ICMEs, it is not a robust signature of STs. Finally, since plasma $\beta \sim 1$, force-free modeling of STs having a magnetic flux rope geometry may be inappropriate.

1. Introduction

Interplanetary coronal mass ejections (ICMEs) and their subset magnetic clouds (MCs) occupy a central place in discussions of the influence of the active Sun on the disturbance level of the terrestrial magnetosphere. This is because these configurations typically possess physical parameters which may reach up to extreme values that last for several hours [see, e.g., *Farrugia et al.*, 1997]. MCs, which are characterized by an above-average magnetic field strength, a large and smooth rotation of the field vector in a plasma of low proton temperature and/or proton beta (T_p and β_p) [*Burlaga et al.*, 1981; *Klein and Burlaga*, 1982], have been modeled as magnetic flux ropes [*Burlaga et al.*, 1981; *Goldstein et al.*, 1983] in a linear force-free approximation [*Burlaga*, 1988; *Lepping et al.*, 1990]. The capabilities of Heliospheric Imagers [*Eyles et al.*, 2009] on STEREO/SECCHI [*Howard et al.*, 2008] to remotely sense these large structures as they erupt from the Sun and propagate through the inner heliosphere allow comparisons with in situ observations. Much effort is being invested in the prediction of the arrival time and in situ properties from remote sensing observations [see, e.g., *Rollett et al.*, 2012; *Möstl et al.*, 2011, and references therein] under various assumptions for the shape of the transients (e.g., The Fixed - Phi [*Kahler and Webb*, 2007] and the Harmonic Mean [*Lugaz et al.*, 2009]). ICME/MC passage at Earth typically lasts for periods of order 1 day giving them a scale size of ~0.30 AU at 1 AU (speed dependent).

Small transients (STs) in the solar wind have also attracted considerable interest, although for different reasons. By "small" we mean configurations whose passage at Earth may last from a few tens of minutes to a few hours. Some of these STs may have the geometry of small magnetic flux ropes. Indeed, attention has also been repeatedly drawn to the presence of small flux ropes in the solar wind [e.g., *Moldwin et al.*, 2000; *Feng et al.*, 2007, 2008; *Cartwright and Moldwin*, 2008, 2010; *Ruan et al.*, 2009]. A main question that has been raised in these studies concerns the possible relation between these STs and the large-scale ICMEs/MCs.

Table 1. Average Values of Key Solar Wind Parameters in 2007–2009 Observed by Wind and ST-A, ST-B

2007–2009	Wind Average	Wind Standard Deviation	ST-A Average	ST-A Standard Deviation	ST-B Average	ST-B Standard Deviation
B (nT)	4.2	2.08	4.34	2.07	3.92	1.98
Proton β	0.95	1.64	0.90	5.94	1.12	1.06
M_A	11.8	6.25	10.7	6.63	11.1	3.33
N_p (cm^{-3})	5.9	4.67	5.58	4.99	4.66	2.16
V_p (km s^{-1})	419	108	410	107	407	20
T_p (K)	8×10^4	7.6×10^4	6.2×10^4	9.8×10^3	6.8×10^4	2.0×10^3
T_e/T_p	3.7	3.10	-	-	-	-

A further, related question concerns their origin: Do STs originate at the Sun or, rather, in heliospheric processes, such as through reconnection at the heliospheric current sheet?

A development which prompted further inquiry into STs is research on the sources of the slow solar wind. In work with SOHO/LASCO coronagraphs, *Sheeley et al.* [1997, 2008] and *Wang et al.* [2000] showed a continuous shedding of small structures from the cusps of coronal streamers. Their lack of a differential speed with respect to the background slow solar wind suggested strongly that these transients form an essential component of the slow solar wind itself. Their orderly kinematics (e.g., a quasi-parabolic dependence of their velocity on height, reaching slow solar wind speeds at ~30 R_S in the outer part of the LASCO C3 field of view, and their similar acceleration) is quite unlike those of the large ICMEs/MCs, whose scatterplot of height versus speed is very irregular [*Sheeley et al.*, 1997, Figure 6].

This work was continued with STEREO, using techniques developed to track the density enhancements in the heliosphere (J maps) [*Sheeley et al.*, 1999, 2008; *Rouillard et al.*, 2008, 2009]. It was shown that stream interaction regions (SIRs) could often entrain STs [*Rouillard et al.* 2009, 2010]. In further work, *Rouillard et al.* [2011] examined six such events, i.e., each entrained in a SIR. Their radial extents were in the range [0.025, 0.118] AU. They were characterized by low plasma beta values, low magnetic field variance, and magnetic field rotations on short timescales. Using J maps to trace the high speed, compressed (dense) stream to the Sun, they were able to demonstrate that these structures generally originated as small mass ejections. One, however, originated as a large mass ejecta, and the authors argued that its small in situ size was due to a spacecraft trajectory which skimmed the larger ejection.

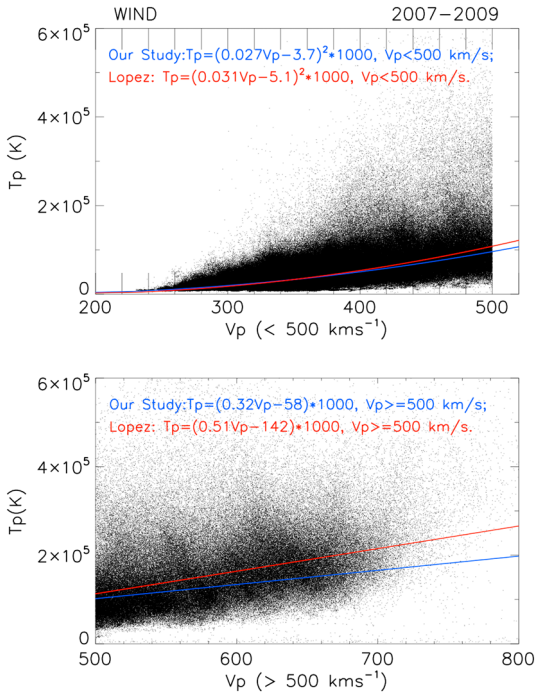

Figure 1. T_p versus solar wind speed V_p in 2007–2009 for (top) slow and (bottom) fast winds. Our least squares fit is shown in blue, and the result derived by *Lopez* [1987] is in red.

A major work on STs in the slow solar wind is that of *Kilpua et al.* [2009], who presented examples seen by the STEREO-A/B (ST-A/B) and Wind probes during Carrington rotations 2054, 2055 (March–April 2007). To search for STs the authors focused on the following features: (i) decreased magnetic field variability, (ii) smooth rotation of the magnetic field, and (iii) clear decreases in T_p and β_p. They found 17 cases in all, some seen at more than one spacecraft. (At this stage of the STEREO mission, the heliographic longitude separation between ST-A and ST-B increased from 1.2 to 5.0°, small enough to permit some multiple observations.) Examples were included where not all of these criteria were simultaneously fulfilled; sometimes only one was satisfied (e.g., see Event 7 in *Kilpua et al.* [2009] and further below). Some had very few of the signatures we associate with large ICMEs and MCs [*Neugebauer and Goldstein*, 1996; *Zurbuchen and Richardson*, 2006; *Richardson and Cane*, 2010]. Using the Global Oscillation Network Group magnetogram-based coronal

Table 2. The Expected Solar Wind T_p as a Function of V_p for 2007–2009: Our Results and Those of *Lopez* [1987]

2007–2009	V_p <500 km s^{-1}		T_{exp} = (A1 × V_p + A2)^2 × 1000		
	V_p ≥500 km s^{-1}		T_{exp} = (B1 × V_p + B2) × 1000		
	A1	σ_{A1}	A2	σ_{A2}	χ^2_A
Our study	0.027	3.1 × 10^{-7}	−3.7	1.2 × 10^{-4}	13,655.2
Lopez	0.031	-	−5.1	-	13,982.4
	B1	σ_{B1}	B2	σ_{B2}	χ^2_B
Our study	0.32	1.3 × 10^{-5}	−58	7.4 × 10^{-3}	37,498.5
Lopez	0.51	-	−142	-	43,111.8

field source surface model map, they found that most of these transients map back to the vicinity of the model sector boundaries. Later, *Kilpua et al.* [2012] studied STs and ICMEs and found that STs occur more often close to SIRs and in the declining phase of fast streams than large ICMEs.

In this paper we carry out a systematic survey of STs during the entire 3 year long, pronounced solar activity minimum 2007–2009. The durations considered are [0.5, 12] h. We do not restrict ourselves to slow solar winds, and we give statistics for slow and fast winds separately.

Our approach is as follows. We first extend *Kilpua et al.*'s [2009] study with the aim of adding other acknowledged ICME/MC signatures also present in their data sets. Essential for this is to compare against the average solar wind properties measured specifically in 2007–2009. From this we find the candidate set of parameters for our survey, i.e., those signatures which recur most frequently in the in situ data of these STs over the two Carrington rotations. These are (i) duration of events between 0.5 and 12 h, (ii) low proton temperature (T_p), (iii) enhanced magnetic field strength (B), (iv) decreased magnetic field variability, (v) coherent field rotations, (vi) low proton beta (β_p), (vii) low Alfvén Mach number (M_A), and (viii) T_e/T_p higher than the average value over the 3 years.

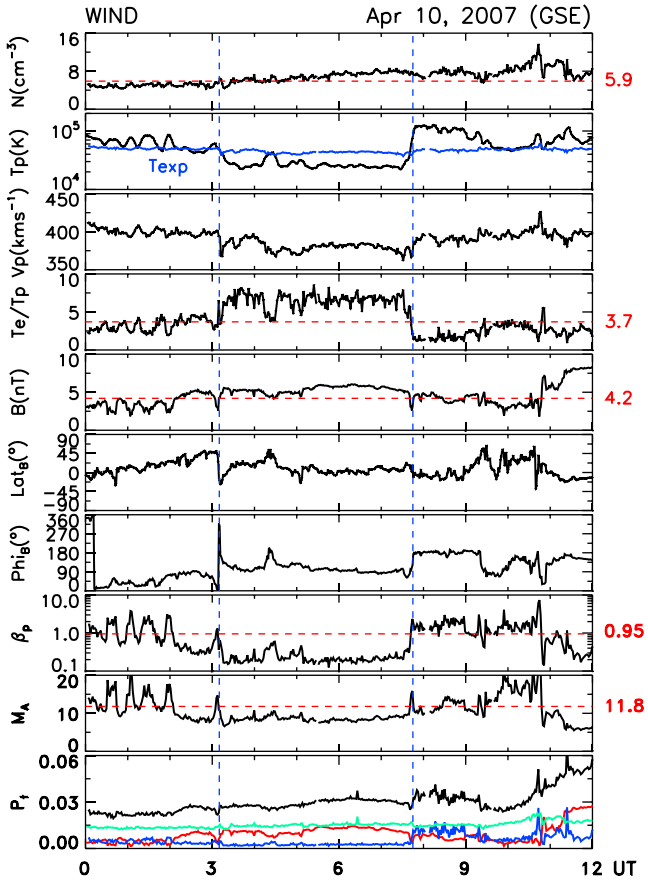

Figure 2. The ST on 10 April 2007, shown between vertical guidelines. For further details, see text.

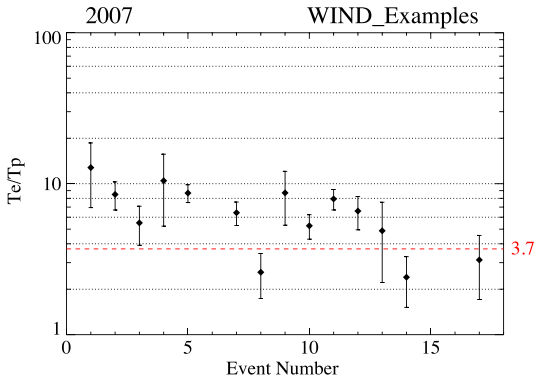

Figure 3. The statistical result for the temperature ratio T_e/T_p for the STs identified by *Kilpua et al.*, [2009] from the Wind spacecraft. The dashed red line labeled 3.7 is the 3 year average of quantity T_e/T_p.

Our definition of STs emerges from this study. We require STs to have durations between 0.5 and 12 h, low T_p and/or low β_p, and an enhanced magnetic field strength relative to the 3 year average. In addition, they must have at least one of the following: (a) decreased magnetic field variability, (b) large, coherent rotation of the field vector, (c) low Alfvén Mach number (M_A), and (d) T_e/T_p higher than the 3 year average. We note that this definition includes small magnetic flux ropes but is not restricted to them.

We then survey by eye the whole 2007–2009 period using Wind key parameter data from the Magnetic Fields Investigation (MFI) [*Lepping et al.*, 1995] and Solar Wind Experiment (SWE) [*Ogilvie et al.*, 1995] instruments. The key parameter data have a temporal resolution of 92 s (plasma) and 1 min (magnetic field). The electron temperature T_e is

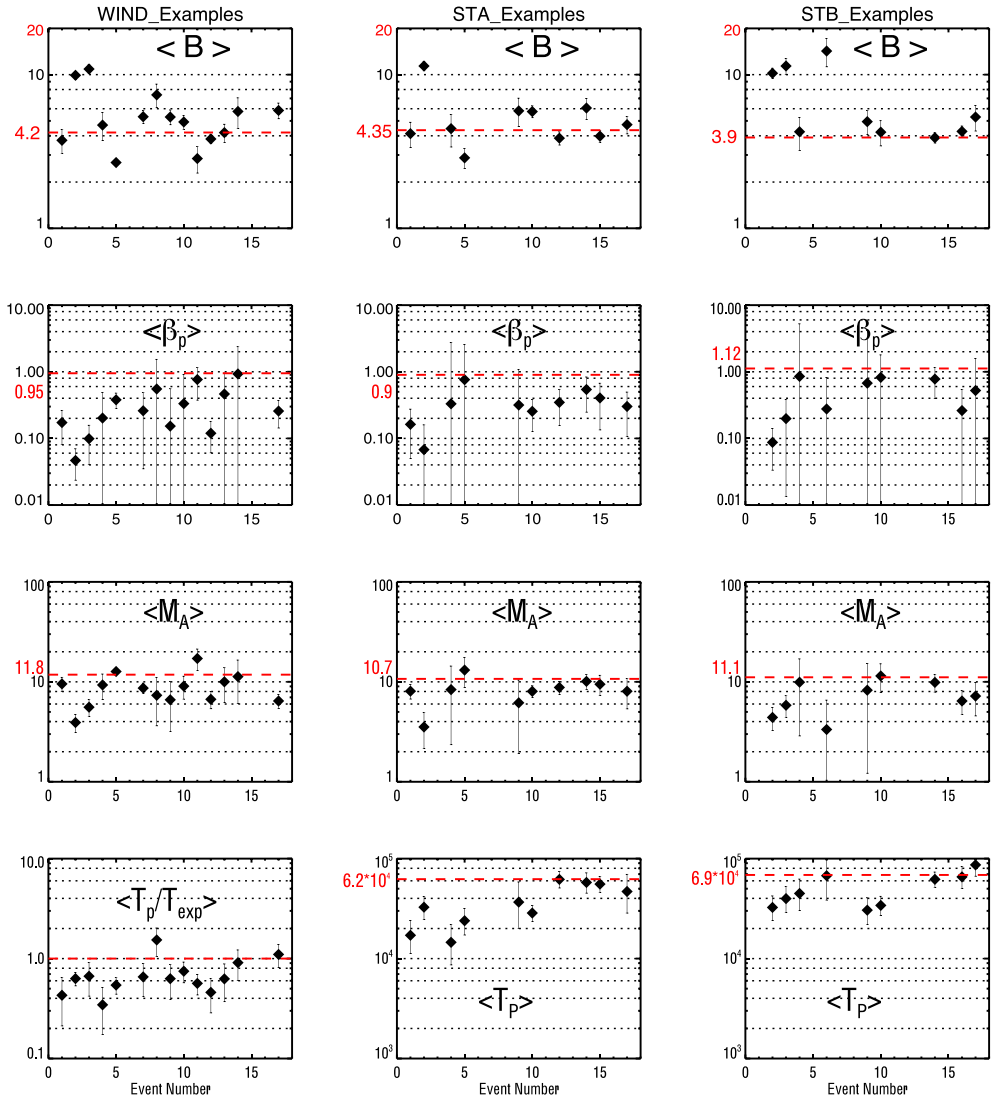

Figure 4. Statistical results on STs in March–April 2007: (a) average B, (b) proton beta, β_p, (c) Alfvén Mach number, M_A, and (d) T_p/T_{exp} as identified by *Kilpua et al.* [2009] from Wind, ST-A, and ST-B. Note that we only plot $< T_p >$ for data from ST-A and ST-B.

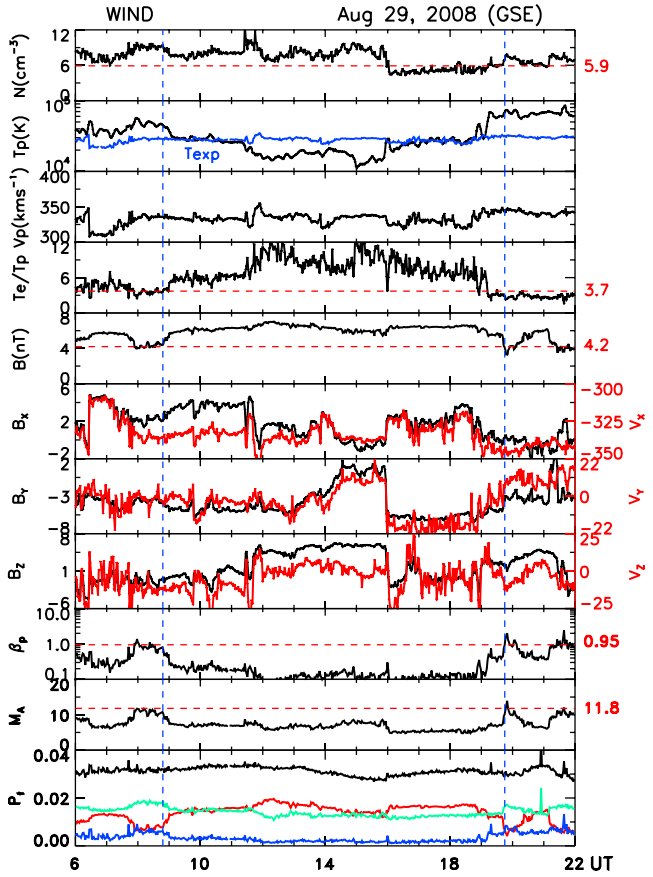

Figure 5. The Alfvénic event on 29 August 2008.

obtained from the SWE instrument at 9 s resolution. We present six events as case studies which we believe to be representative of various features seen in these STs, e.g., where they occur, typical durations, etc. We then present our statistical results, grouping by slow/fast winds. Finally, in section 5, we compare ST properties with those of ICMEs seen during the same period after the tabulation of *Richardson and Cane* [2010].

We stress again that when comparing ST properties to those of the "normal" solar wind we use as reference the solar wind during 2007–2009, which was in many respects (e.g., low magnetic field strength and low plasma density) different from solar winds during minima of other solar cycles [*Smith and Balogh*, 2008; *McComas et al.*, 2008; *Farrugia et al.*, 2012]. This information is given in Table 1, which includes the average values and the standard deviations of the (i) magnetic field, B; (ii) β_p; (iii) M_A; (iv) proton density, N_p; (v) proton bulk speed, V_p; (vi) T_p; and (vii) T_e/T_p of the solar wind. The average magnetic field strength in these 3 years was only 4.2 nT (Wind), while 4.34 nT and 3.92 nT were obtained from the ST-A and ST-B data sets, respectively. The expected proton temperature for normal solar wind expansion, however, depends on the solar wind bulk flow speed. Empirical formulas obtained from statistics were given by *Lopez* [1987]. However, we do this from first principles. The reason for doing so is that the period under study had special properties, and we want to be sure that these are adequately reflected in the statistics.

2. Selection Procedure and Methodology

In this section we motivate our selection criteria for STs by extending the work of *Kilpua et al.* [2009], isolating other indicators which appear frequently in the data sets. We give one example to illustrate the approach. We also discuss the expected proton temperature of the solar wind during 2007–2009, useful for comparison purposes.

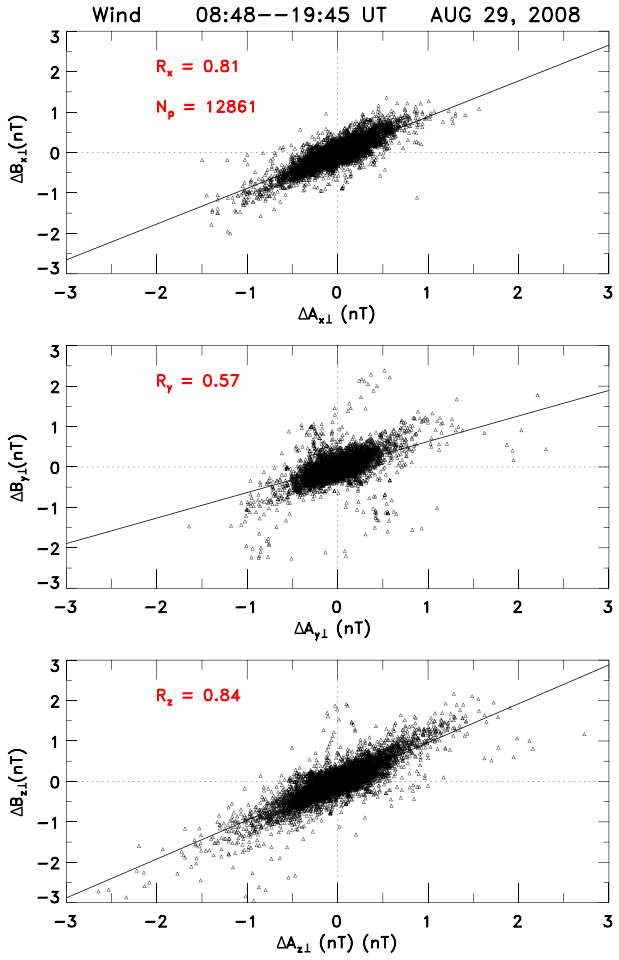

Figure 6. For the Alfvén event on 29 August 2008. For further details, see text.

We begin with the latter. We derive the expected T_{exp} of the solar wind in 2007–2009 as a function of V_p. The statistical formula obtained by *Lopez* [1987] is

$$T_{exp} = (0.031 \times V_p - 5.1)^2 \times 1000 \quad \text{for} V_p < 500 \text{kms}^{-1};$$

$$T_{exp} = (0.51 \times V_p - 142) \times 1000 \quad \text{for} V_p \geq 500 \text{kms}^{-1}.$$

We shall assume a similar functional form for T_{exp} in terms of V_p and also use the same demarcation line at V_p = 500 km s^{-1}. The key parameter data from the Wind/SWE instrument results in over 9 × 10^5 data points in the 3 year period (720271 in slow, and 209379 in fast wind). We used the Interactive Data Language least squares fitting routine "curvefit", and the initial parameters were set very different from those of *Lopez* [1987]. The routine then converges to

$$T'_{exp} = (0.027 \times V_p - 3.665)^2 \times 1000 \quad \text{for} V_p < 500 \text{kms}^{-1};$$

$$T'_{exp} = (0.323 \times V_p - 58.277) \times 1000 \quad \text{for} V_p \geq 500 \text{kms}^{-1}.$$

Figure 1 shows these results in blue. The red trace shows the *Lopez* [1987] values. The goodness of fit parameter $Ø^2$ is shown in Table 2. As can be seen, the results we obtain are close to those of Lopez and, particularly for the slow solar wind, the fits almost coincide.

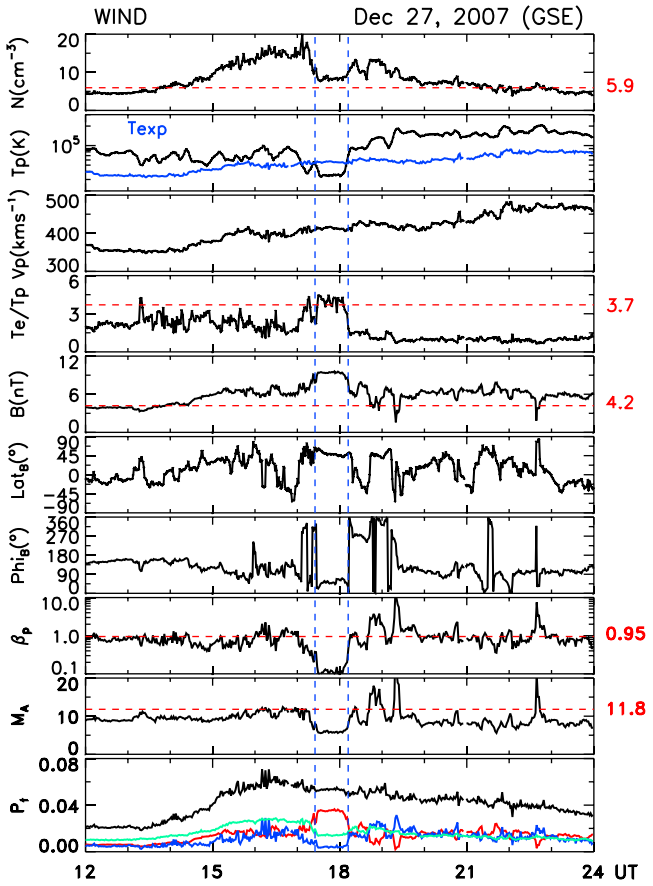

Figure 7. The ST on 27 December 2007, shown between vertical guidelines. (top to bottom) The proton density, temperature (in blue: the expected temperature in year 2007–2009), bulk speed, the T_e/T_p temperature ratio, the total field and its latitude and longitude in GSE coordinates, the β_p, the M_A, and the pressures (black: total; red: magnetic; blue: proton; green: electron thermal pressure).

We looked at the 17 events listed by *Kilpua et al.* [2009], which occurred in March–April 2007. We added the following quantities in search of possible further candidate signatures of ST: (i) T_e/T_p and (ii) Alfvén Mach number, M_A. The reason for including (i) is that in various studies it has been shown that in large transients (ICMEs/MCs) $T_e >> T_p$ [*Fainberg et al.*, 1996; *Richardson et al.*, 1997; *Sittler and Burlaga*, 1998]. Indeed, this ratio could reach values of ~10 [*Sittler and Burlaga*, 1998]. In an example using Ulysses data, *Osherovich et al.* [1999] showed values >20 at large heliospheric distances. The Alfvén Mach number, M_A, is typically lower in ICMEs and MCs than in the surrounding solar wind [*Farrugia et al.*, 1995; *Lavraud et al.* 2007; *Leitner et al.*, 2009, 2010]. Indeed, low M_A is one reason magnetosheath properties, and hence solar wind-magnetosphere interactions, can depart strongly from typical behavior when ICMEs pass Earth, because it implies enhanced magnetic forces acting on the sheath flow [*Farrugia et al.*, 1995; *Lavraud and Borovsky*, 2008].

To illustrate our selection procedure, we look at a ST on 10 April 2007 (event No. 7) from *Kilpua et al.*'s [2009] list. Figure 2 shows, from top to bottom, N_p, T_p, V_p, the temperature ratio T_e/T_p, the total magnetic field strength, B, the latitude and longitude of the magnetic field (GSE coordinates), the β_p, M_A, and the pressures, P (black trace: total, red: magnetic, blue: proton, green: electron thermal pressure). The horizontal red traces in the various panels indicate the average value of the respective quantities in 2007–2009. The blue trace in the second panel is the expected proton temperature for normal solar wind expansion as derived above.

The ST interval, lasting ~4.5 h, is bracketed by the vertical guidelines in Figure 2. From the second panel it is seen that the proton temperature T_p is well below the expected temperature. Indeed, this is the way this particular ST was identified in the original work. But there are other signatures satisfying our criteria for a ST: proton β_p is << 1 and the T_e/T_p temperature ratio clearly rose to well above average values (6.43 ± 1.13; mean and standard deviation). The total magnetic field strength was ~5.3 nT ± 0.27 nT. At 1 AU 5.3 nT is not usually considered a strong solar wind field. However, the 3 year average is 4.2 nT (red line). Similar

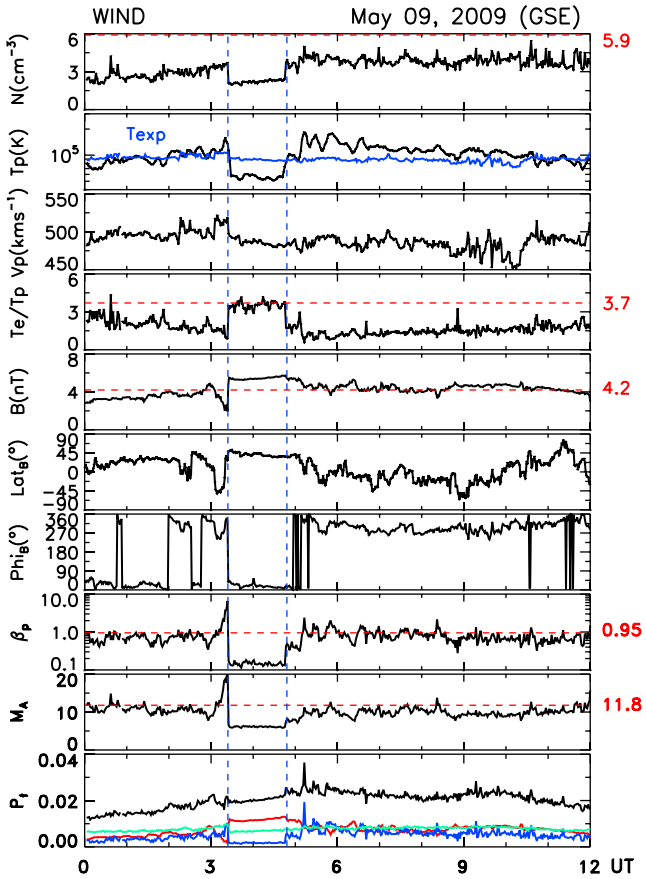

Figure 8. The ST on 9 May 2009. The format is the same as that of Figure 7.

arguments apply to M_A (last-but-one panel). Its average value in this ST is 8.7, while in the 2007–2009 solar wind the average value was 11.8 (Table 1), so it is lower than average. Except for the low T_p, which was chosen to be one of the most important criteria in Kilpua et al.'s work, there are four other properties which can distinguish this ST event from the ambient solar wind.

We now consider the total ensemble of 14 events seen at Wind during these two Carrington rotations. First, we show results on the temperature ratio T_e/T_p (Figure 3), plotting the mean values and the standard deviations for each event. The red dashed line gives the 3 year average. The range of values extends over [~2.5, ~14]. It is evident that in many cases this temperature ratio exceeds the average value over 2007–2009. So this temperature ratio may be a good indicator of STs.

Figure 4 shows scatterplots of the results obtained for the parameters we consider. The three columns refer, from left to right, to Wind (14 STs), ST-A (10 STs), and ST-B (9 STs) observations, respectively. Plotted in rows from top to bottom are (a) the average field strength B, (b) the average β_p, (c) the average M_A, and (d) the average $T_p/T_{\exp}$. For the STs observed by ST-A and ST-B, we compare the proton temperature T_p with the average values. Standard deviations are shown by the vertical lines.

Wind. Concerning the average B in STs, we have values in the range [~3, ~11] nT. So clearly this quantity, as noted also by *Kilpua et al.* [2009], is generally, but not always, above average values of the solar wind at 1 AU. When comparing with the 3 year average of 4.2 nT (red dashed line), many STs (86%) have indeed a higher average field strength. The average proton beta ($< \beta_p >$) in STs varies over a wide range, and some have large standard deviations. However, it is clear that a $\beta_p < 1$ is a recurrent feature of these STs. The average M_A values lie in the range [4, 20]. Since the mean of the 2007–2009 measurements of this quantity is 11.8 ± 6.25 (Table 1; horizontal line), most STs (86%) have an average M_A which is lower than that in the solar wind in this 3 year period. The average T_p/T_{exp} is with two exceptions below unity. For those STs with $T_p < T_{exp}$, the difference between T_p and T_{exp} is not that large. This point will be taken up again in section 5.

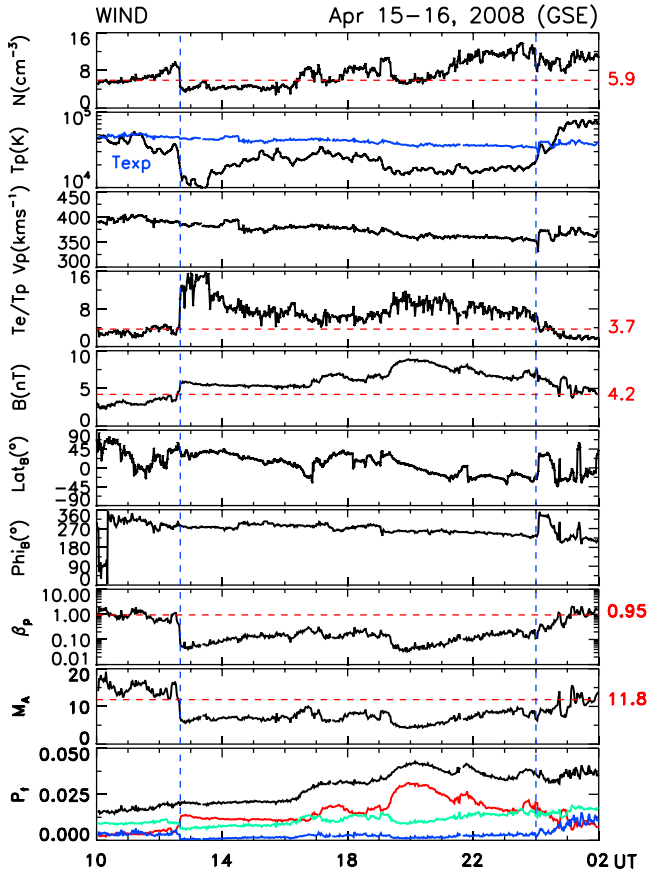

Figure 9. Case event 3 (15–16 April 2008) with data plotted in a format similar to that of Figure 7.

ST-A and ST-B. Similar trends are seen in the ST-A and ST-B examples. Most STs have an average magnetic field stronger than the average value. Quantity β_p <1 is also a reliable parameter in these examples. Most of the STs have mean M_A below the normal solar wind value. In the last panel we compare the proton temperature with the surroundings. We find that the average proton temperatures at ST-A and ST-B are 6.2 $\times$ 10^4 K and 6.8 $\times$ 10^4 K, respectively. In ST-A, all the events have T_p < 6.2 $\times$ 10^4 K, and most of them (8 out of 10) have T_p > 2.4 $\times$ 10^4 K. A similar result can be seen in ST-B, where almost all the STs (8/9) have T_p lower than its average value, and all T_p higher than 2.4 $\times$ 10^4 K (thermal speed, v_{th} = 20 km s^{-1}). The above analysis motivated our choice of characteristics we shall use to identify STs, detailed in section 1.

3. STs in 2007–2009: Case Event Studies

In this section we present a number of case studies to illustrate the varieties of ST features and the ambient conditions they occur in.

3.1. Alfvénic Fluctuations

We start first with the kind of event we exclude. As pointed out by *Marubashi et al.* [2010] and *Cartwright and Moldwin* [2010], some solar wind Alfvénic structures can be mistaken for STs. For that reason we examined all events we identified to remove those which were evidently Alfvénic fluctuations. We give one example in Figure 5, which was observed by Wind on 29 August 2008. From top to bottom the panels show the proton density N_p, temperature T_p (in blue: the expected temperature for normal solar wind from the statistics discussed above), bulk speed, the T_e/T_p temperature ratio, the total field, the magnetic field vector in GSE Cartesian coordinates (B_x, B_y, B_z), and overlaid in red, the corresponding solar wind velocity components, β_p; M_A; and the total pressures (red: magnetic; blue and green: proton and electron thermal pressures, respectively; black: total).

Part of the Alfvénic event is bracketed by two vertical guidelines and lasts from 08:48 to 19:45 UT. We find this event to have (i) decreased T_p, at least in the central part (~11:30–16:00 UT); (ii) enhanced T_e/T_p (> 3.7);

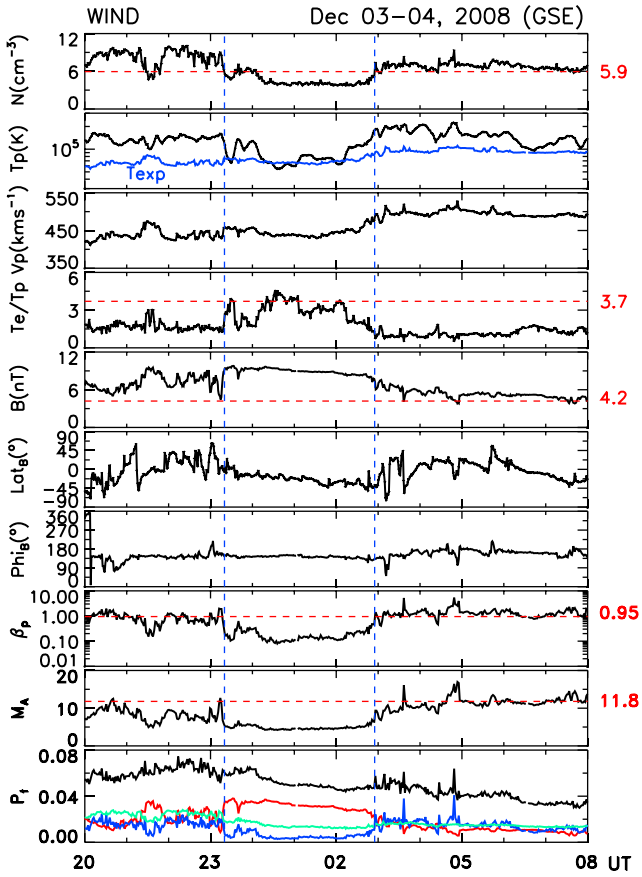

Figure 10. Case event 4 on 3 December 2008. Similar format as in Figure 7.

(iii) stronger-than-average magnetic field strength; and (iv) low β_p ($\beta_p < 1$) and low M_A ($M_A < 11.8$). All these properties comply with our definition of STs. However, when we compare the components of the magnetic field and the velocity vectors (GSE coordinates; overlaid in red with scales on the right), we see a clear correlation between them. That means that the event is really an Alfvénic structure.

We confirm this formally by comparing in Figure 6 the perturbations of the magnetic field perpendicular to the background field ($\Delta\mathbf{B}_\perp$) with the perturbations of the velocity perpendicular to the background magnetic field and modified by a function of the mass density ρ ($\Delta\mathbf{A}_\perp \equiv (\mu_0\rho)^{1/2}\Delta\mathbf{V}_\perp$). The background field is obtained from a seven-point running average of the magnetic field data. The regression lines are shown. With correlation coefficients of 0.8, 0.6, 0.8 (x, y, z), over 12,861 data points, the correlation is good. These are thus Alfvén waves propagating against (positive gradient) the magnetic field. We carried out this procedure on all the events we initially identified. If the regression coefficients were larger than 0.5 for all three components, we classified them as Alfvénic events.

3.2. Event 1: 27 December 2007

We now discuss six case studies to present what we think are representative features of the STs listed in this paper. The first event was observed by Wind on 27 December 2007. Figure 7 shows the plasma and magnetic field data. From top to bottom, the panels show the proton density, temperature T_p (in blue: the statistically expected value in 2007–2009), the proton bulk speed, the T_e/T_p temperature ratio, the total field and the latitude and longitude of the magnetic field vector in GSE coordinates, proton β_p, M_A, and the total pressures (black: total; red: magnetic; blue: proton; green: electron thermal pressure). The red horizontal lines indicate the 3 year averages of the respective quantities (Table 1). The event is shown between the two vertical lines.

This is a very short duration ST, lasting only 47 min. Features of this event are the low proton temperature ($< T_p > /T_{exp} = 0.65$) and the low proton β_p (~ 0.13). The average magnetic field strength ($< B > = 9.2$ nT) is about twice the average value, and the average M_A (~6.0) is about one half of average (red line). The field

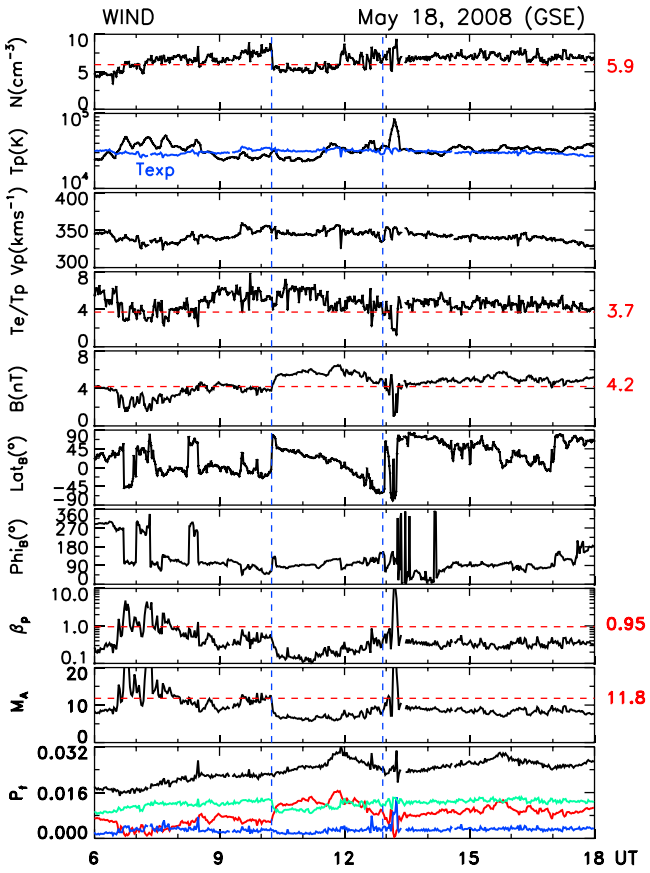

Figure 11. Case event 5 (18 May 2008). Similar format as in Figure 7.

variability is lower than in the surroundings. The T_e/T_p ratio, while it reaches above ambient values in the 12 h interval shown, is just 1.03 times the 3 year average. The event occurs within a stream-stream interaction region (positive gradient in V_p), but has a constant V_p, implying no radial expansion. The variations of the latitude and longitude of the magnetic field are small. It is in approximate pressure balance ($P_t = 0.053 \pm 0.001$ nPa). The event starts and ends with strong gradients in N_p, T_p, B, and T_e/T_p, distinguishing it clearly from the ambient solar wind. Using the average speed of 413 km s^{-1} and the duration gives a rough estimate of the scale size in the Sun-Earth direction of 0.0078 AU (183 R_E, Earth radii).

3.3. Event 2: 9 May 2009

Figure 8 shows the second case, which was observed on 9 May 2009. The data of this and the other four case studies are shown in the same format as that of Figure 7. This ST is encountered in the time interval 03:24 to 04:48 UT (between vertical guidelines). The following properties may be seen: (i) the proton temperature, T_p/T_{exp} is 0.65, as in case 1; (ii) an average field strength which is higher the 3 year average ($< B > = 5.4$ nT); (iii) low magnetic field variability; (iv) a low β_p (~0.16), and (iv) a lower M_A (6.2) than the surroundings, and about one half of its 3 year average value (11.8).

The event occurs in a (borderline) fast solar wind. The decreasing trend in the flow profile indicates radial expansion, with a value for the expansion velocity of ~ 15 km s^{-1}. (The expansion velocity is computed as $(V_f - V_r)/2$, where V_f (V_r) are the velocities of the front (rear) boundaries of the structure). As in event 1, there are sharp gradients in the parameters at both the front and rear boundaries, which appear to be discontinuities. The pressures reflect the increasing trends in the density and field strength. For this event, too, the T_e/T_p, while it is clearly enhanced compared to ambient values plotted in the figure and helps to distinguish it from them, does not exceed the 3 year average (ratio = 3.5 ± 0.2 versus 3.7). As in the first event the proton density is depressed during the event. Its value (2.3 ± 0.34 cm^{-3}) is lower than ambient, and it is also much lower than the average value (5.9 cm^{-3}) over these 3 years. This feature is similar to that of the first event.

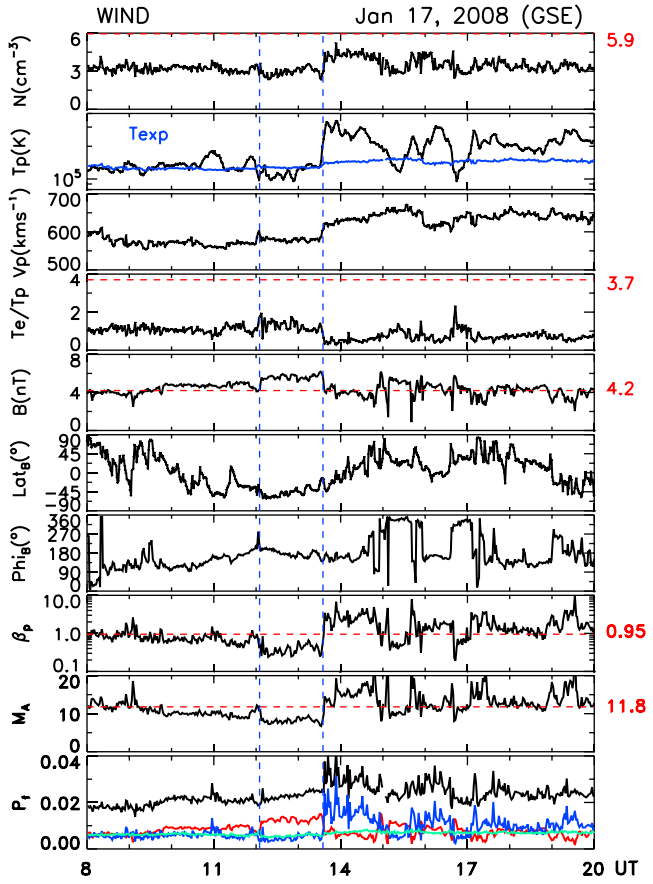

Figure 12. Case event 6: 17 January 2008.

This ST is only 1.4 h long. Multiplying by an average speed of 486 km s^{-1}, we obtain a scale size in the Sun-Earth direction of approximately 0.016 AU (2.45 $\times$ 10^6 km) (376 R_E).

At 5.44 $\pm$ 0.13 nT, the magnetic field B in this event is very steady. There is a decreased variability of the field compared to the surroundings. Since B is much steadier than its components, the (small) fluctuations are likely perpendicular to the background field. There is an interesting feature adjoining the front boundary of

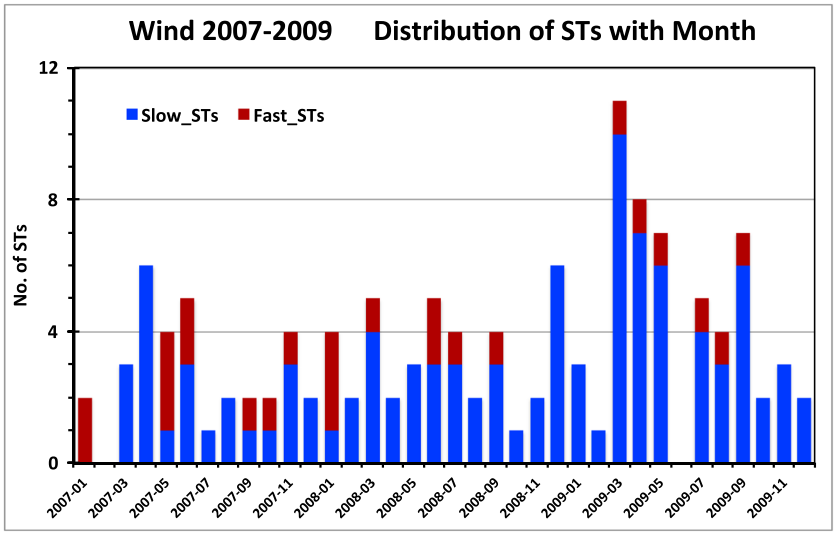

Figure 13. The distribution of number of STs per month observed by Wind in 2007–2009.

Table 3. Distribution of STs in the Slow Solar Wind

Year	Percentage of Slow Solar Wind	Percentage of Slow ST
2007	60%	70%
2008	55%	80%
2009	89%	87%

this small transient, namely, a strong double depression of the magnetic field and a concomitant rise in M_A and β_p. This might be a signature of reconnection, but we do not discuss this further here.

3.4. Event 3: 15 April 2008

In contrast to the previous two examples, the third ST observed on 15 April 2008 is a long event, lasting 11.3 h (Figure 9). It lies in the slow wind (average 371 km s^{-1}). The properties of this event are (i) the proton temperature ($< T_p > = 2 \times 10^4$K) is lower than the expected temperature, (ii) the T_e/T_p ratio is high, reaching a value of 16.4, well above the 3 year average; (iii) the average magnetic field strength (6.5 nT) is higher than the 3 year average (4.2 nT); (iv) the β_p is very low (~0.13 $\pm$ 0.06); and (v) low M_A, ~7.02 $\pm$ 1.29.

The smooth decrease of the proton velocity from 380 km s^{-1} to 350 km s^{-1} indicates a radial expansion speed of 15 km s^{-1}. The latitude of the magnetic field exhibits a large rotation (~70°), though it is not monotonic, and the longitude of the magnetic field rotates by ~50°. Discontinuous changes in many field and plasma parameters are present, especially at the leading edge.

3.5. Event 4: 3 December 2008

Another event is the one observed on 3–4 December 2008 (Figure 10). It is characterized by (i) a magnetic field strength (~8.91 $\pm$ 0.52 nT) which is about twice the 3 year average; (ii) low magnetic field variance; (iii) low β_p (0.19); and (iv) low M_A (4.9). In this event, too, the proton density ($< N_p > = 4.5$ cm^{-3}) drops below ambient values. The T_p/T_{exp} fluctuates and is often above unity.

With an average bulk speed ~447 km s^{-1}, and a duration of 3.58 h, the scale size of this event at L1 point is about 0.039 AU (916 R_E). The event is embedded in a stream-stream interaction region (overall change in V is 35 km s^{-1}), as the solar wind flow changes from slow to fast.

In this event the leading speed $\leq$ trailing edge speed, which is indicative of radial contraction. Though the T_e/T_p does not generally exceed the 3 year average, it has values forming a clear local enhancement. The latitude of the magnetic field changes smoothly by about 45°, while its longitude is very steady in this period. It may thus be considered as a small magnetic flux rope.

3.6. Event 5: 18 May 2008

An example of a ST with clear magnetic flux rope features is the one observed on 18 May 2008 (Figure 11). Its duration is ~ 2.67 h. The magnetic field executes a large and coherent north-south rotation of 135°. The longitude remains relatively steady at 90°. The event occurs in the slow solar wind and is being convected with the surrounding flow. With a low-proton beta ($< \beta_p > = 0.22$), and a stronger-than-average magnetic

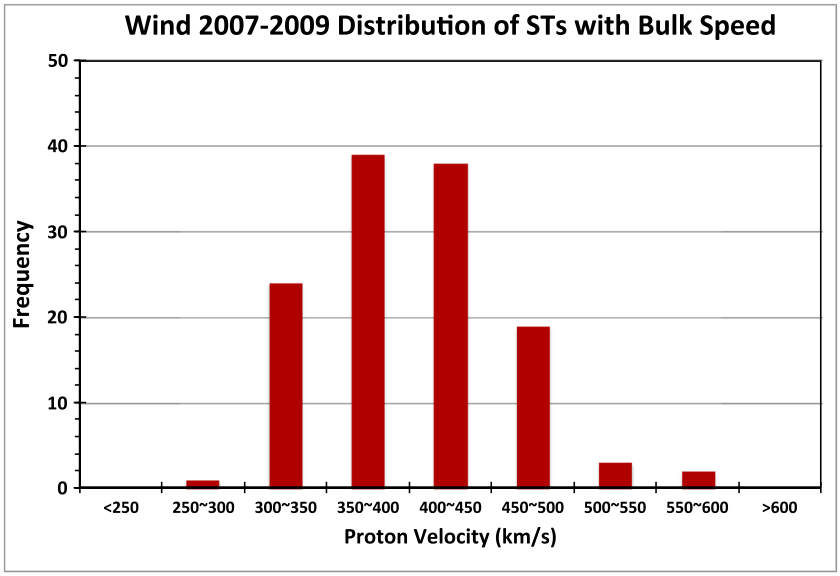

Figure 14. The proton velocity distribution of the observed STs.

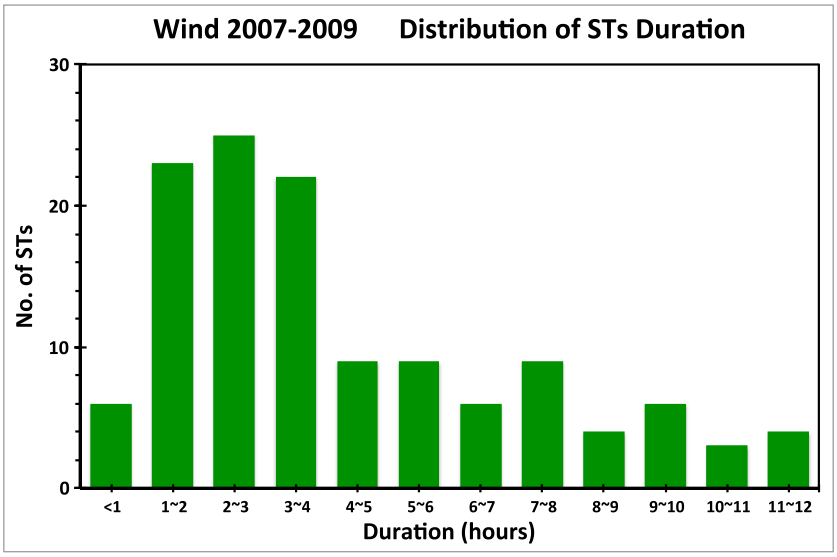

Figure 15. The distribution of ST duration.

field strength (5.5 versus 4.2 nT), it may be considered as a small magnetic cloud. Interestingly, however, the T_p/T_{exp} ratio fluctuates around unity as in the surrounding plasma. Further, T_e/T_p, while above the 3 year average, is hardly distinguishable from the surroundings. A rough estimate of the diameter of the ST is ~0.022 AU (517 R_E). Noteworthy are the pressure profiles, where it can be seen that the sum of the thermal pressures (electron + proton) is of the same order as the magnetic pressure. Thus, it is not a priori clear that such a flux rope may be modeled as a force-free configuration.

3.7. Event 6: 17 January 2008

The last example was observed on 17 January 2008, data for which are shown in Figure 12. This ST is being convected (no gradient in V_p) with the fast ($< V_p > = 580$ km s^{-1}) solar wind. Again, as in the previous example, it satisfies all the criteria for a small MC, with an enhanced field strength, smooth rotation in both field latitude and longitude, and a low β_p. However, as in the previous example, T_p is hardly different from expected values. The pressure profiles again indicate a substantial contribution of the thermal pressures to the total. T_e/T_p was only 1.26, i.e, much lower than the 3 year average (3.7).

4. Statistical Survey

We now present statistical results from our survey, considering first the ST occurrence rate. Figure 13 shows a histogram of the number of STs per month as a function of time. In all we identified (by eye) 126 STs, with 33 STs in the year 2007, 40 STs in 2008, and 53 STs in 2009. On average we thus find 3.5 events/month. It appears that in 2009 the STs are more frequent. This may be due to the fact that in 2009 the slow solar wind occurred over a larger fraction of the time (89%). The fraction of fast STs in year 2007 is much higher than in the other 2 years. The percentages of the slow solar wind in each year and the percentages of the slow STs are listed in the Table 3.

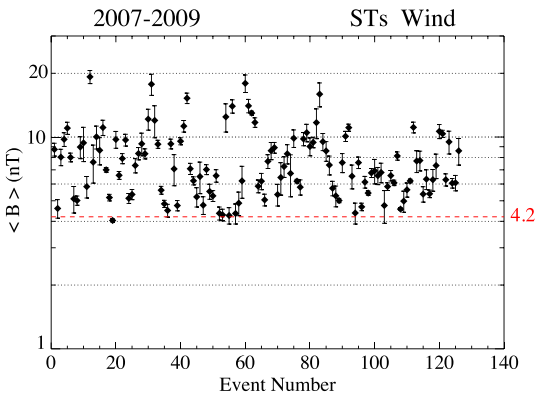

Figure 16. The statistical result of the average B in the 126 STs. The value 4.2 nT is the 3 year average.

Figure 14 sorts these events by average speed. Most of the events have average bulk speeds in the range [300, 500]. Of the 126 STs, 102 STs (81%) are in the slow solar wind (<450 km s^{-1}).

The distribution of the durations is shown in Figure 15. The most frequently observed ST

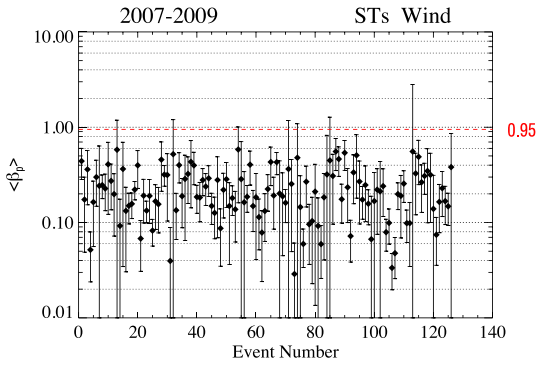

Figure 17. The statistical result of the average proton beta, β_p.

duration lies between 1 and 4 h. The average duration of the 126 STs is ~4.3 h, and 94 STs (75%) last less than 6 h.

We now turn to the distribution of individual parameters.

1. Average magnetic field (Figure 16). In STs we find that this quantity lies in [4, 20 nT]. The ensemble average is ~7.8 nT ± 3.0 nT, i.e., about twice the 3 year average (4.2 nT). This conclusion can only be drawn if we compare with average properties of the solar wind in 2007–2009, as we do (see section 1).
2. β_p. Figure 17 show average β_p per event and their standard deviations. All lie below the 3 year value and are confined to the range [0.02, 0.7], albeit with large standard deviations. The ensemble average of β_p is 0.24, about 4 times smaller than the 3 year average (0.95). Grouping by solar wind speed, the average β_p = 0.235 (slow) and 0.249 (fast), i.e., there is no significant difference between the slow and fast solar wind.
3. M_A. Figure 18 shows that the averages of this quantity lie in [~2, 12]. The ensemble average $< M_A >$ is 6.3 (about one half of 3 year average). In slow solar wind $< M_A >$ is 6.29, and in fast solar wind is 6.50.
4. T_e/T_p. Figure 19 shows that for almost all the STs, the temperature ratio $T_e/T_p > 1$ and lies in a band of [0.9, ~20]. The ensemble average for all STs is 4.31. It is 4.64 and 3.02 for the slow and fast solar winds, respectively. The average temperature ratio in our study is only a little higher than the 3 year value (3.7). The implications of (ii) and (iv) are discussed further in the last section.
5. T_p/T_{exp}. The scatterplot of Figure 20 shows that this ratio straddles the 3 year average. In 53% of cases, this ratio is below, and in 47% it is above, unity. Thus, while $T_p << T_{exp}$ is often considered a very robust signature of the ICMEs [*Gosling et al.*, 1973; *Richardson and Cane*, 1995], it is not a robust signature of STs. This point is considered further in the section 5.

5. Summary and Discussion

We have discussed properties and distributions of small solar wind transients (STs) during 2007–2009. They were monitored by the SWE and MFI instruments on Wind. We elaborated a methodology of how to search for these events. We first extended the analysis of *Kilpua et al.*, [2009] covering two consecutive Carrington rotations with the aim of including other parameters which may be of interest. Having identified these quantities, we arrived at a selection scheme for STs. This scheme included, but was not restricted to, magnetic flux ropes. After eliminating Alfvénic fluctuations, we found 126 examples of STs. They were of various durations but mostly shorter than 6 h. The majority were found in the slow solar wind and convecting with it. It was a major concern of our effort to compare ST properties with those of the background solar wind in these 3 years which, as has been pointed out in previous studies, had unusual properties, such as low magnetic field strengths and low proton densities.

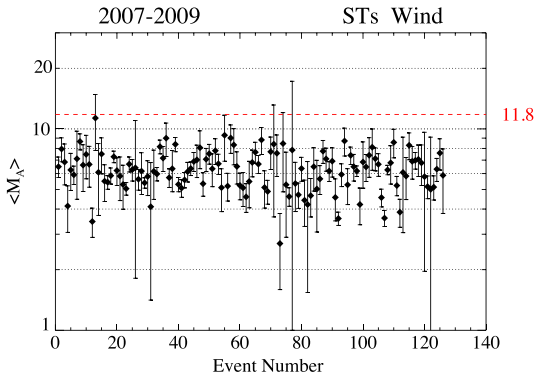

Figure 18. The statistical result of M_A.

Some caveats on the selection are in order. When searching by eye for these transients, we sometimes had difficulty in locating their exact boundaries. When the boundaries were very unclear, we did not include the event. Note also that by definition we excluded events which are shorter than 30 min. Thus, the set of STs we arrived at is nonexclusive: It is not being claimed that we found them all. Worth noting is also that identification of STs depends on the definition. We paid particular care to this, but other works may use similar but not identical definitions.

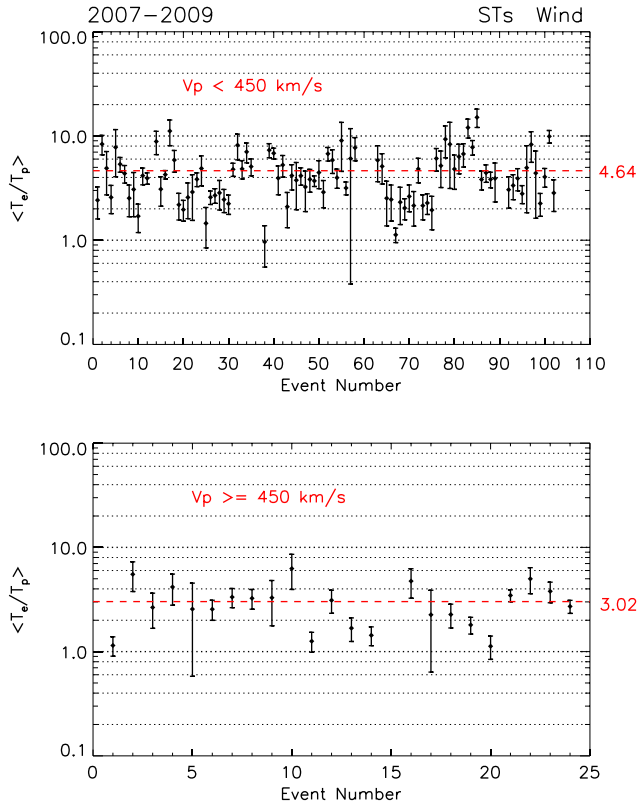

Figure 19. Statistical result for the temperature ratio T_e/T_p sorted by solar wind speed. (top) Slow wind and (bottom) fast wind. The red dashed lines are the respective ensemble averages.

We now take a closer look at our results for the temperature ratio T_e/T_p. This is hardly ever discussed in connection with STs (but see *Yu et al.* [2013]). And yet it has been discussed in connection with large-scale ICMEs (see references in section 1 and below). Locally, T_e/T_p in STs is generally well above ambient values. Indeed, this ratio alone can often distinguish STs from their surroundings (see, for example, the case studies 2 and 4). However, overall, it fluctuated around the 3 year average of this ratio (Figure 19).

For the normal solar wind, *Newbury et al.* [1998] gave a rule-of-thumb estimate for the value of T_e based on an analysis of ISEE data. They reached the conclusion that irrespective of solar wind speed, a good estimate of T_e is $T_e = 1.42 \times 10^5$ K. Figure 21 shows T_e for our 3 year period. Its average value is 1.51×10^5 K, which is in very good agreement with Newbury et al.'s result. This is remarkable seeing that Newbury et al.'s study covered 18 months when ISEE 3 was orbiting the L1 point during a phase approaching solar maximum of cycle 21. Below we shall compare the temperature ratio T_e/T_p in STs with that in ICMEs during the solar minimum 2007–2009.

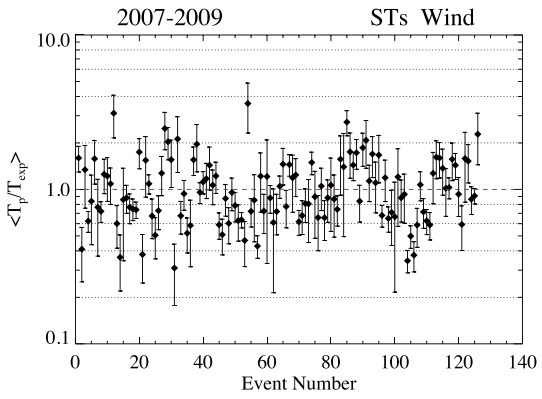

Figure 20. The statistical result for T_p/T_{exp}.

The local high value of T_e/T_p in STs has an important implication. It concerns force-free modeling of those STs which have the geometry of magnetic flux ropes, i.e., those which exhibit a large and coherent rotation of the magnetic field vector. When this temperature ratio is taken into account, the plasma β (electrons + protons + α particles, though we did not study the α's in this paper) will of course rise substantially. Figure 22 confirms this result over our assembly. We use here measured values of T_e and not the average value. At an average value of 0.85 ± 0.38, the plasma β is not

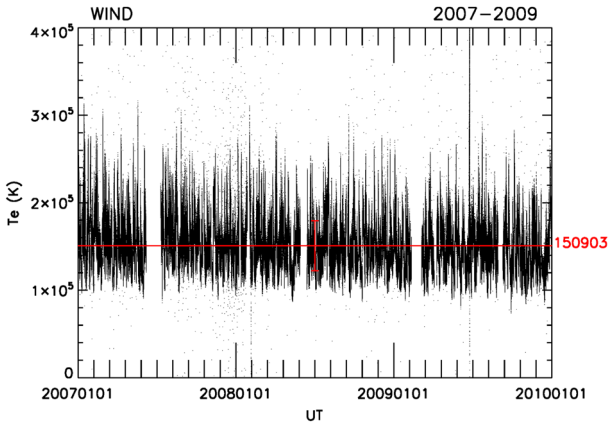

Figure 21. Temporal profile of the electron temperature T_e. In red, the mean value and its standard deviation.

small, and thus, the thermal pressure is comparable to the magnetic pressure. Alphas would also increase the plasma β by a few percent in the slow wind and perhaps by up to 20% in the fast wind. This means that force-free modeling for flux-rope STs might not be a suitable approach. Grad-Shafranov reconstruction and the elliptical model of *Hidalgo et al.* [2002] could be more suited.

An interesting feature often seen in our STs were the sharp gradients at one or both boundaries. Sometimes these were abrupt enough to become discontinuities. The possibility of some of these being rotational discontinuities, implying reconnection with the ambient plasma, will be followed up in future work.

Perhaps the most distinguishing feature of STs is that, generally, they do not expand but convect with the solar wind. This eliminates adiabatic cooling and yields a T_p distribution which straddles the expected T_p value (see Figure 20). (See below when we compare with the properties of ICMEs in this period.) It will emerge that while a low T_p has been universally considered as a very robust signature of ICMEs, it is not a robust signature of STs.

The convection with the solar wind and the general occurrence of STs in the slow wind lends support to the idea that many STs represent the plasma blobs which *Sheeley et al.* [1999] discovered to be emanating steadily from streamer cusps. And blobs tracked directly in the Imagers are the most direct way of associating STs with streamer transients [e.g., *Rouillard et al.*, 2011]. See *Kilpua et al.* [2012] for an in-depth investigation of this issue. However, further work is required to determine all possible origin(s) of STs, such as statistical studies of their densities and the properties of α particles and heavier ions.

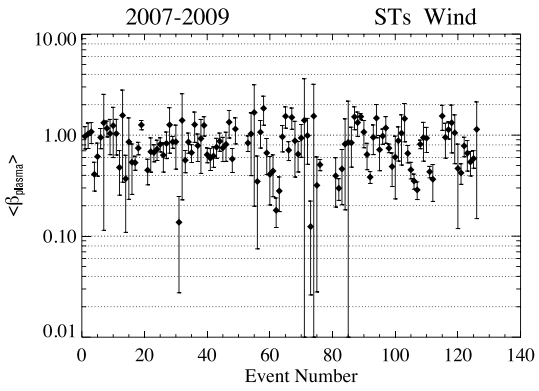

Figure 22. Statistics of the plasma β (electrons + protons) over the 126 STs. Values generally cluster around unity.

We now compare our results for STs with the properties of ICMEs in this same period. We use for the latter the compilation of *Richardson and Cane* [2010], who tabulated 15 ICMEs. Summary results are collected in Figure 23. Proceeding by column, this shows the average (a) B, (b) M_A, (c) β_p, (d) T_e/T_p, and (e) T_p/T_{exp}. Comparing with the corresponding plots for STs, it may be seen that (i) B is similar in STs and (ii) so is M_A. By contrast, (iii) β_p is lower and (iv) T_p/T_{exp} is lower (0.67 in ICMEs versus 1.1 in STs, Table 4) and perhaps in part as a consequence of this, (v) average T_e/T_p is higher (~8.3) in ICMEs. Values of T_e/T_p ~10 were also obtained in various studies on ICMEs/MCs. The strength of the resulting ion acoustic wave emissions can be seen very trenchantly in an example from Ulysses where $T_e/T_p \approx 20$ [see *Osherovich et al.*, 1999, Figures 4b and 4c]. In summary, it seems that the major difference between in situ observations of ICMEs and STs is the proton temperature and its effects on other derived parameters. It is lower than T_{exp} in ICMEs but of the same order in STs.

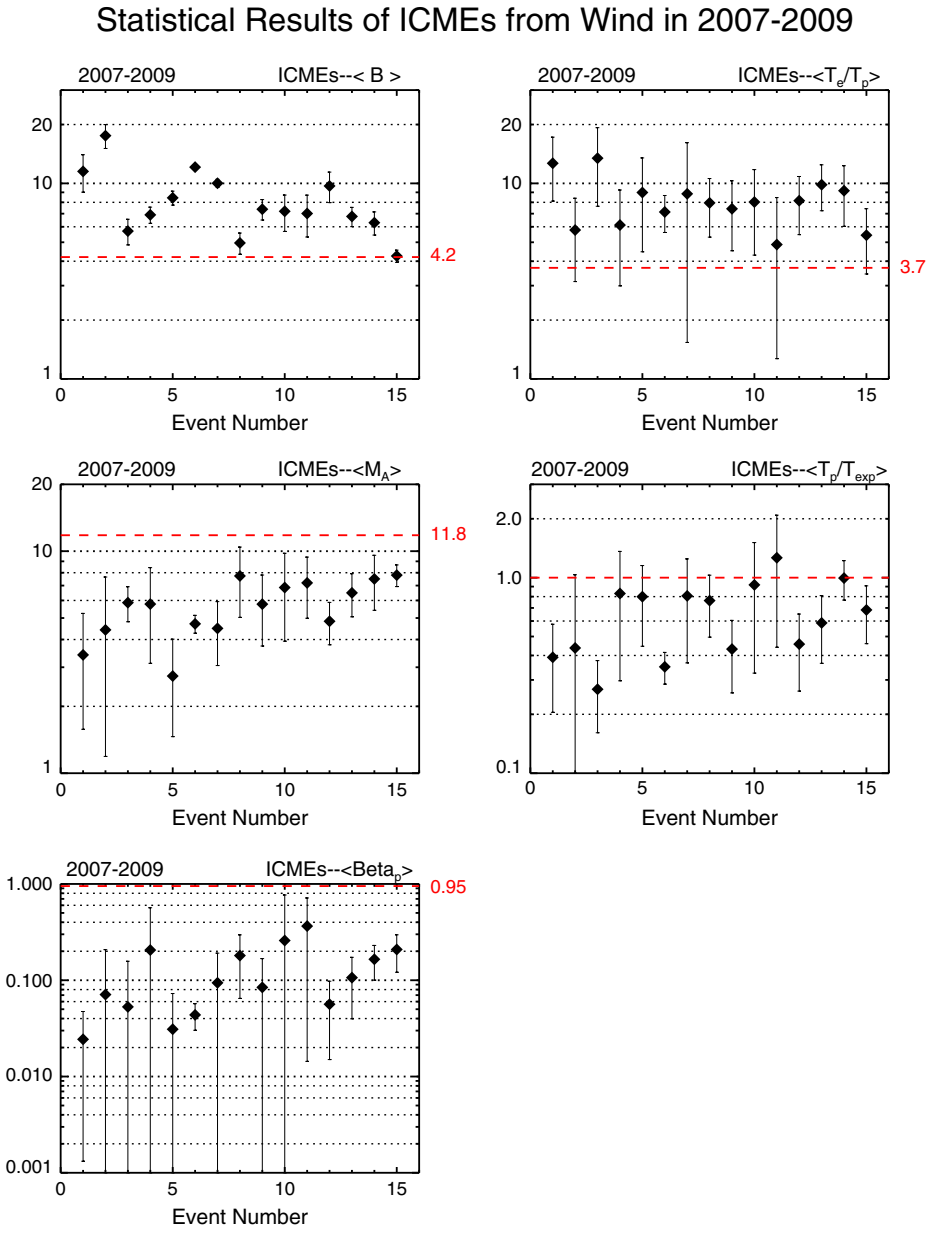

Figure 23. Statistical results for the ICMEs observed by Wind in 2007–2009 from the classification of *Richardson and Cane* [2010].

Table 4. Comparison of STs and ICMEs in 2007–2009

2007–2009	STs	ICMEs
$< B >$	7.84 ± 3.00	8.39 ± 3.40
$< \beta_p >$	0.24 ± 0.13	0.13 ± 0.10
$< M_A >$	6.3 ± 1.4	5.7 ± 1.6
$< T_e/T_p >$	4.3 ± 2.5	8.3 ± 2.4
$< T_p/T_{exp} >$	1.10 ± 0.56	0.67 ± 0.28

As a last item, we consider in Figure 24 the distribution of the expansion velocity, V_{exp} for STs (blue) and ICMEs (red). Some STs have negative V_{exp}, implying compression. This might reflect the fact that if encountered in SIRs, they are often compressed by the trailing faster stream. The mean and standard deviations are as follows: $V_{exp}^{ST} = -3.8 \pm 15.2$ km s^{-1} and $V_{exp}^{ICME} = 9.9 \pm 17.1$ km s^{-1}. Thus, during the 3 year minimum, the expansion speeds are not large, though the average V_{exp} for STs are significantly smaller. If we take only positive values in Figure 24, we obtain 17.3 km/s for ICMEs and 8.0 km/s for STs.

Recall that with only 15 ICMEs, the statistics are not so robust. So we depart from practice and consider a larger ICME data set, one that encompasses 14 years and all solar activity levels taken from *Richardson and*

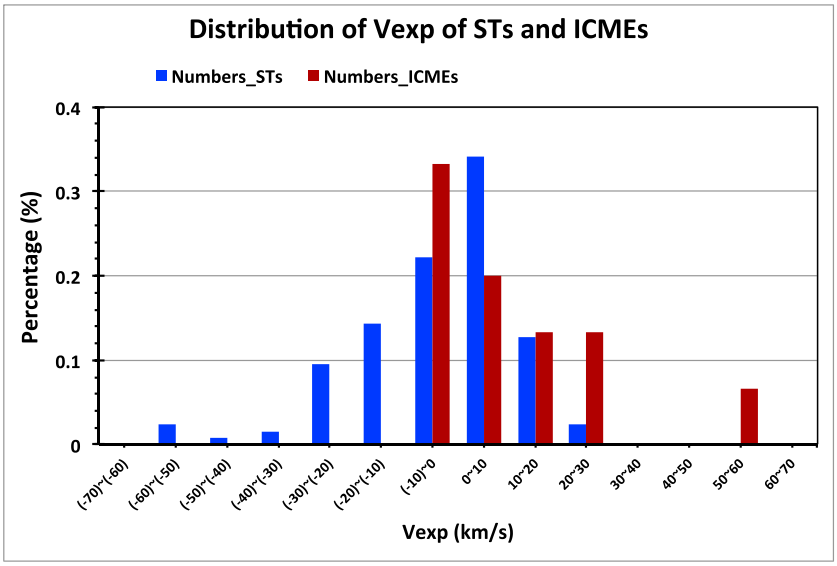

Figure 24. Normalized distribution of the expansion velocity for STs (in blue; 126 cases) and ICMEs (in red; 15 cases).

Cane [2010]. For the V_{exp} of ICMEs they find 31 km/s and 42 km/s with, and without, negative values included. (Other authors quoted in Richardson and Cane find even higher values). It seems that indeed ICMEs expand considerably more than STs. Currently, this is only based on a limited data set, but we intend to extend to a larger data set in future work.

Acknowledgments

This work was supported by NASA grants NNX12AH45G, NNX13AP39G, and NNX09AG28G, NSF grant AGS-1140211, and STEREO/PLASTIC grant to UNH. This research was supported by a Marie Curie International Outgoing Fellowship with the 7th European Community Framework Programme. The work has received funding from the Seventh Framework Program (FP7/2007–2013) under grant 263252 [COMESEP]. Work supported also by NASA grant NNX13AP52G.

Philippa Browning thanks Marcia Neugebauer and an anonymous reviewer for their assistance in evaluating this paper.

References

Burlaga, L., E. Sittler, F. Mariani, and R. Schwenn (1981), Magnetic loop behind an interplanetary shock: Voyager, Helios and IMP-8 observations, *J. Geophys. Res.*, *86*(A8), 6673–6684.

Burlaga, L. F. (1988), Magnetic clouds and force-free fields with constant alpha, *J. Geophys. Res.*, *93*(A7), 7217–7224.

Cartwright, M. L., and M. B. Moldwin (2008), Comparison of small-scale flux rope magnetic properties to large-scale magnetic clouds: Evidence for reconnection across the HCS?, *J. Geophys. Res.*, *113*, A09105, doi:10.1029/2008JA013389.

Cartwright, M. L., and M. B. Moldwin (2010), Heliospheric evolution of solar wind small-scale magnetic flux ropes, *J. Geophys. Res.*, *115*, A08102, doi:10.1029/2009JA014271.

Eyles, C. J., et al. (2009), The heliospheric imagers onboard the STEREO mission, *Solar Phys.*, *254*, 387–445.

Fainberg, J., V. A. Osherovich, R. G. Stone, R. J. MacDowall, and A. Balogh (1996), Ulysses observations of electron and proton components in a magnetic cloud and related wave activity, *AIP Conf. Proc. Solar Wind*, *8*, 554–557.

Farrugia, C. J., N. V. Erkaev, H. K. Biernat, and F. Burlaga (1995), Anomalous magnetosheath properties during Earth passage of an interplanetary magnetic cloud, *J. Geophys. Res.*, *100*, 19,245–19,257.

Farrugia, C. J., L. F. Burlaga, and R. P. Lepping (1997), Magnetic clouds and the quiet-storm effect at Earth, *Geophys. Monogr.*, *98*, 91–106.

Farrugia, C. J., et al. (2012), Deep solar activity minimum 2007–2009: Solar wind properties and major effects on the terrestrial magnetosphere, *Solar Phys.*, *281*, 461–489.

Feng, H. Q., D. J. Wu, and J. K. Chao (2007), Size and energy distributions of interplanetary magnetic flux ropes, *J. Geophys. Res.*, *112*, A02102, doi:10.1029/2006JA011962.

Feng, H. Q., D. J. Wu, C. C. Lin, J. K. Chao, L. C. Lee, and L. H. Lyu (2008), Interplanetary small- and intermediate-sized magnetic flux ropes during 1995–2005, *J. Geophys. Res.*, *113*, A12105, doi:10.1029/2008JA013103.

Goldstein, H. (1983), On the field configuration in magnetic clouds, *Solar Wind Five, NASA Conf. Publ*, *2280*, 731–733.

Gosling, J. T., V. Pizzo, and S. J. Bame (1973), Anomalously low proton temperatures in the solar wind following interplanetary shock waves—Evidence for magnetic bottles *J. Geophys. Res.*, *78*, 2001–2009.

Hidalgo, M. A., T. Nieves-Chinchilla, and C. Cid (2002), Elliptical cross-section model for the magnetic topology of magnetic clouds, *Geophys. Res. Lett*, *29*(13), 15-1–15-4, doi:10.1029/2001GL013875.

Howard, R. A., et al. (2008), Sun Earth Connection Coronal and Heliospheric Investigation (SECCHI), *Space Sci. Rev.*, *136*, 67–115.

Kahler, S. W., D. F. Webb (2007), V arc interplanetary coronal mass ejections observed with the Solar Mass Ejection Imager, *J. Geophys. Res.*, *112*, A09103, doi:10.1029/2007JA012358.

Kilpua, E. K. J., et al. (2009), Small solar wind transients and their connection to the large-scale coronal structure, *Solar Phys.*, *256*, 327–344.

Kilpua, E. K. J., L. K. Jian, Y. Li, J. G. Luhmann, and C. T. Russell (2012), Observations of ICMEs and ICME-like solar wind structures from 2007–2010 using near-Earth and STEREO observations, *Solar Phys.*, *281*, 391–409.

Klein, L. W., and L. F. Burlaga (1982), Interplanetary magnetic clouds at 1 AU, *J. Geophys. Res.*, *87*(A2), 613–624.

Lavraud, B., J. E. Borovsky, A. J. Ridley, E. W. Pogue, M. F. Thomsen, H. Rème, A. N. Fazakerley, and E. A. Lucek (2007), Strong bulk plasma acceleration in Earth's magnetosheath: A magnetic slingshot effect? *Geophys. Res. Lett.*, *34*, L14102, doi:10.1029/2007GL030024.

Lavraud, B., and J. E. Borovsky (2008), Altered solar wind-magnetosphere interaction at low Mach numbers: Coronal mass ejections, *J. Geophys. Res.*, *113*, A00B08, doi:10.1029/2008JA013192.

Leitner, M., C. J. Farrugia, A. Galvin, K. D. C. Simunac, H. K. Biernat, and V. A. Osherovich (2009), The solar wind quasi-invariant observed by STEREO A and B at solar minimum 2007 and comparison with two other minima, *Solar Phys.*, *259*, 381–388.

Leitner, M., and C. J. Farrugia (2010), Solar wind quasi invariant within ICMEs, *AIP Conf. Proc., Solar Wind*, *12*, 652–654.

Lepping, R. P., J. A. Jones, and L. F. Burlaga (1990), Magnetic field structure of interplanetary magnetic clouds at 1 AU, *J. Geophys. Res.*, *95*(A8), 11957–11965.
Lepping, R. P., et al. (1995), The wind magnetic field investigation, *Space Sci. Rev.*, *71*, 207–229.
Lopez, R. E. (1987), Solar cycle invariance in solar wind proton temperature relationships, *J. Geophys. Res.*, *92*, 11,189–11,194.
Lugaz, N., A. Vourlidas, and I. I. Roussev (2009), Deriving the radial distances of wide coronal mass ejections from elongation measurements in the heliosphere—Application to CME-CME interaction, *Ann. Geophys.*, *27*, 3479–3488.
Marubashi, K., K. S. Cho, and Y. D. Park (2010), Torsional Alfvén waves as pseudo magnetic flux ropes, *AIP Conf. Proc., Solar Wind*, *12*, 240–244.
McComas, D. J., R. W. Ebert, H. A. Elliott, B. E. Goldstein, J. T. Gosling, N. A. Schwadron, and R. M. Skoug (2008), Weaker solar wind from the polar coronal holes and the whole Sun, *Geophys. Res. Lett.*, *35*, L18103, doi:10.1029/2008GL034896.
Möestl, C., et al. (2011), Arrival time calculation for interplanetary coronal mass ejections with circular fronts and application to STEREO observations of the 2009 February 13 eruption, *Astrophys. J.*, *741*, 34.
Moldwin, M. B., S. Ford, R. Lepping, J. Slavin, and A. Szabo (2000), Small-scale magnetic flux ropes in the solar wind, *Geophys. Res. Lett.*, *27*, 57–60.
Neugebauer, M., and R. Goldstein (1996), Particle and field signatures of coronal mass ejections in the solar wind, *Geophys. Mon. Ser.*, *99*, AGU.
Newbury, J. A., C. T. Russell, J. L. Phillips, and S. P. Gary (1998), Electron temperature in the ambient solar wind: Typical properties and a lower bound at 1AU, *J. Geophys. Res.*, *103*, 9553–9566.
Ogilvie, K. W., et al. (1995), SWE, a comprehensive plasma intrument for the WIND spacecraft, *Space Sci. Rev.*, *71*, 55–77.
Osherovich, V. A., J. Fainberg, and R. G. Stone (1999), Multi-tube model for interplanetary magnetic clouds, *Geophys. Res. Lett.*, *26*, 401–404.
Richardson, I. G., and H. V. Cane (1995), Regions of abnormally low proton temperature in the solar wind (1965–1991) and their association with ejecta, *J. Geophys. Res.*, *100*, 23,397–23,412.
Richardson, I. G., C. J. Farrugia, and H. V. Cane (1997), A statistical study of the behavior of the electron temperature in ejecta, *J. Geophys. Res.*, *102*, 4691–4699.
Richardson, I. G., and H. V. Cane (2010), Near-Earth interplanetary coronal mass ejections during solar cycle 23 (1996–2009): Catalog and summary of properties, *Solar Phys.*, *264*, 189–237.
Rollett, T., C. Moëstl, M. Temmer, A. M. Veronig, C. J. Farrugia, and H. K. Biernat (2012), Constraining the kinematics of coronal mass ejections in the inner heliosphere with in-situ signatures, *Solar Phys.*, *276*, 293–314.
Rouillard, A. P., et al. (2008), First imaging of corotating interaction regions using the STEREO spacecraft, *Geophys. Res. Lett.*, *35*, L10110, doi:10.1029/2008GL033767.
Rouillard, A. P., et al. (2009), A multispacecraft analysis of a small-scale transient entrained by solar wind streams, *Solar Phys.*, *256*, 307–326.
Rouillard, A. P., et al. (2010), Intermittent release of transients in the slow solar wind: 1. Remote sensing observations, *J. Geophys. Res.*, *115*, A04103, doi:10.1029/2009JA014471.
Rouillard, A. P., et al. (2011), The solar origin of small interplanetary transients, *Astrophys. J.*, *734*, 7.
Ruan, P., A. Korth, E. Marsch, B. Inhester, S. Solanki, T. Wiegelmann, Q.-G. Zong, R. Bucik, and K.-H. Fornacon (2009), Multiple-spacecraft study of an extended magnetic structure in the solar wind, *J. Geophys. Res.*, *114*, A02108, doi:10.1029/2008JA013769.
Sittler, E. C., Jr., and L. F. Burlaga (1998), Electron temperatures within magnetic clouds between 2 and 4 AU: Voyager 2 observations, *J. Geophys. Res.*, *103*, 17,447–17,454.
Sheeley, N. R., Jr., et al. (1997), Measurements of flow speeds in the corona between 2 and 30 $R_{\odot}$, *Astrophys. J.*, *484*, 472–478.
Sheeley, N. R. Jr., J. H. Walters, Y.-M. Wang, and R. A. Howard (1999), Continuous tracking of coronal outflows: Two kinds of coronal mass ejections, *J. Geophys. Res.*, *104*, 24,739–24,767.
Sheeley, N. R., Jr., et al. (2008), Heliospheric images of the solar wind at Earth, *Astrophys. J.*, *675*, 853–862.
Smith, E. J., and A. Balogh (2008), Decrease in heliospheric magnetic flux in this solar minimum: Recent Ulysses magnetic field observations, *Geophys. Res. Lett.*, *35*, L22103, doi:10.1029/2008GL035345.
Wang, Y.-M., N. R. Sheeley Jr., D. G. Socker, R. A. Howard, and N. B. Rich (2000), The dynamical nature of coronal streamers, *J. Geophys. Res.*, *105*, 25,133–25,142.
Yu, W., et al. (2013), Small solar wind transients: Stereo-A observation in 2009, *AIP Conf. Proc., Solar Wind*, *13*, 311–314.
Zurbuchen, T. H., and I. G. Richardson (2006), In-situ solar wind and magnetic field signatures of interplanetary coronal mass ejections, *Space Sci. Rev.*, *123*, 31–43.